Published online 13 April 2008

Nucleic Acids Research, 2008, Vol. 36, No. 9 ***3139–3149***
doi:10.1093/nar/gkn143

Structure and function of the regulatory C-terminal HRDC domain from *Deinococcus radiodurans* RecQ

Michael P. Killoran and James L. Keck*

Department of Biomolecular Chemistry, University of Wisconsin School of Medicine and Public Health, Madison, WI 53706-1532, USA

Received November 7, 2007; Revised March 12, 2008; Accepted March 14, 2008

ABSTRACT

RecQ helicases are critical for maintaining genome integrity in organisms ranging from bacteria to humans by participating in a complex network of DNA metabolic pathways. Their diverse cellular functions require specialization and coordination of multiple protein domains that integrate catalytic functions with DNA–protein and protein–protein interactions. The RecQ helicase from *Deinococcus radiodurans* (DrRecQ) is unusual among RecQ family members in that it has evolved to utilize three 'Helicase and RNaseD C-terminal' (HRDC) domains to regulate its activity. In this report, we describe the high-resolution structure of the C-terminal-most HRDC domain of DrRecQ. The structure reveals unusual electrostatic surface features that distinguish it from other HRDC domains. Mutation of individual residues in these regions affects the DNA binding affinity of DrRecQ and its ability to unwind a partial duplex DNA substrate. Taken together, the results suggest the unusual electrostatic surface features of the DrRecQ HRDC domain may be important for inter-domain interactions that regulate structure-specific DNA binding and help direct DrRecQ to specific recombination/repair sites.

INTRODUCTION

RecQ proteins are DNA unwinding enzymes (helicases) with critical roles in maintaining genomic integrity in organisms from every kingdom of life (1). Mutations in three of the five human *recQ* genes have been identified as the causes of Bloom's, Werner's and Rothmund–Thomson syndromes (2–4). These syndromes are characterized by susceptibility to several rare cancers and, in the case of Werner's and Rothmund–Thomson's syndromes, developmental defects and premature aging. The severe consequences of these diseases reflect the critical roles of RecQ helicases in genome maintenance processes such as DNA replication, recombination and repair. Research in a variety of model systems continues to reveal the extensive co-dependencies of genome metabolic pathways and the role of RecQ proteins in maintaining genomic integrity through their interactions with a diverse number of proteins and nucleic acid structures (1,5). The relatively simple bacterial RecQ family members provide desirable resources for dissection of the biochemical and structural features that govern RecQ's cellular functions.

The bacterium *Deinococcus radiodurans* is an excellent model system for studying the roles of RecQ proteins in genome maintenance. While organisms such as *Escherichia coli*, *Saccharomyces cerevisiae*, mice and humans can survive modest amounts of γ-irradiation [less than a few hundred Grey (Gy)], *D. radiodurans* can survive doses as high as 5000 Gy without a loss of viability (6). γ-Radiation is a particularly lethal DNA damaging agent due to its ability to induce DNA double-strand breaks (DSBs) during exposure; DSBs are difficult to mend as they leave no template behind for directing DNA repair. Surprisingly, identifiable homologs for the *recB* and *recC* genes that encode the major DSB repair machinery in *E. coli* are not found in *D. radiodurans* (7). This implicates a distinct recombinational repair pathway (similar to the RecF pathway from *E. coli*) as being central to maintaining genomic integrity in *D. radiodurans*, as homologs for all of its genes have been identified. In *recBC*$^-$ *E. coli*, RecF pathway activation requires mutation in the *sbcB* gene, which encodes a 3′–5′ exonuclease that is also conspicuously absent from the *D. radiodurans* genome (8). In the RecF pathway in *E. coli*, RecQ initiates repair by unwinding duplex DNA in the 3′–5′ direction, while the single-stranded DNA (ssDNA) exonuclease RecJ hydrolyzes the 5′ strand and the RecA-mediator proteins RecF, RecO and RecR load RecA onto the 3′ strand to drive homologous recombination (9–11). It remains unclear, however, the way in which *D. radiodurans* may have extended its use of a RecF-like pathway and its constituents to a greater extent in repairing DNA damage.

The unusual domain architecture of the RecQ protein from *D. radiodurans* could help address this question. The configuration of conserved domains found in almost

*To whom correspondence should be addressed. Tel: +1 608 263 1815; Fax: +1 608 262 5253; Email: jlkeck@wisc.edu

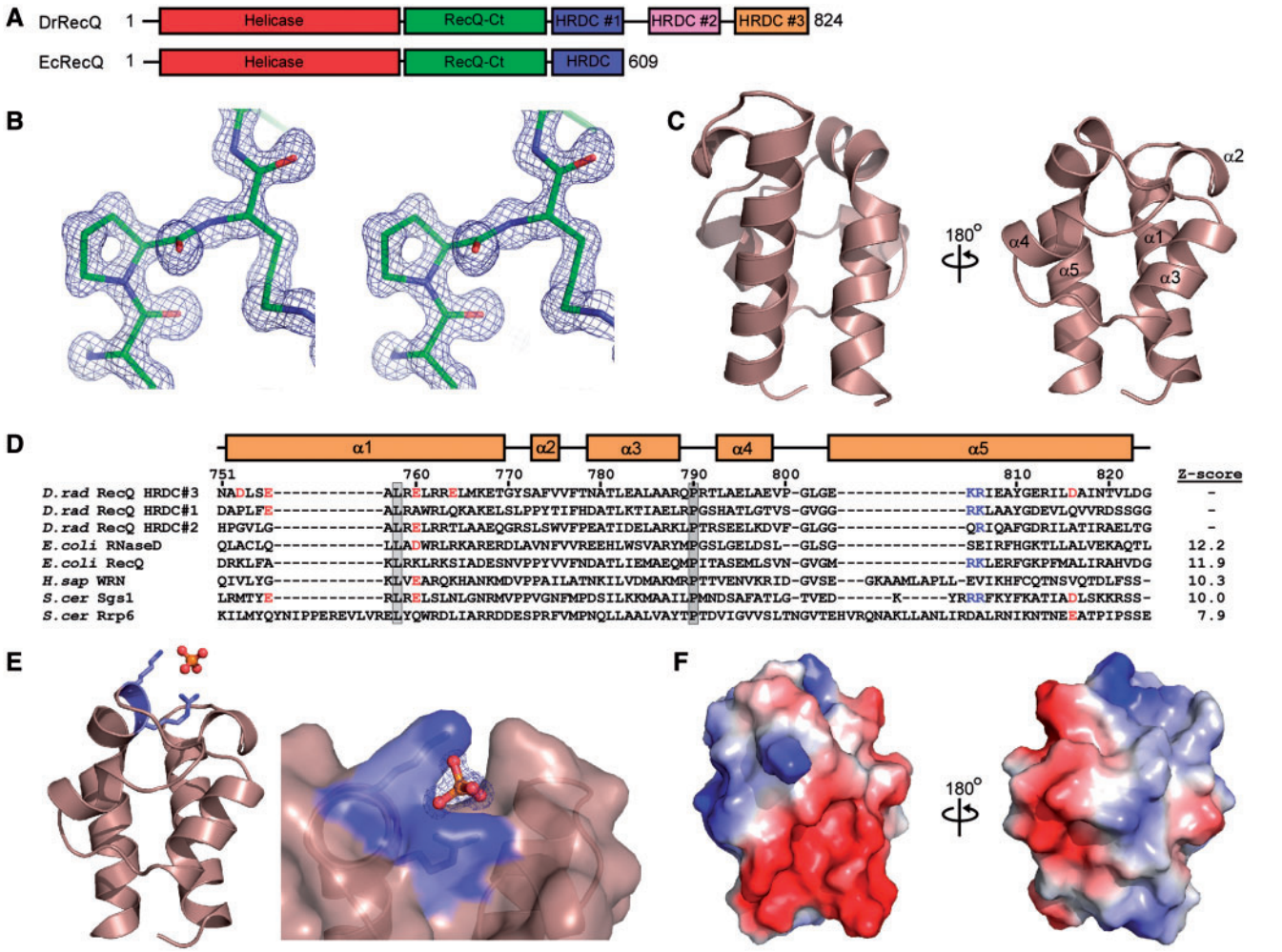

Figure 1. Structural features of *D. radiodurans* RecQ HRDC #3. (**A**) Schematic comparison of the conserved domains of DrRecQ and EcRecQ. Each protein is comprised of a Helicase, RecQ-Ct and HRDC domain. DrRecQ features two additional HRDC domains at its C-terminus numbered HRDC #2 and #3, respectively. (**B**) Stereodiagram of the $2F_o-F_c$ electron density map surrounding P790 in the α3 to α4 loop contoured at 2.0 σ. All structural figures were created using PyMol (39). (**C**) The α-helical fold of HRDC #3 shown as ribbons. Helix numbers are included in the representation on the right. (**D**) Sequence alignment of DrRecQ HRDC domains and HRDC #3's closest structural homologs. The secondary structure and corresponding residue numbers in DrRecQ are indicated at the top of the alignment. Structural homologs were identified using the DALI search engine (34) and resulting *Z*-scores are shown following each sequence. Basic residues contacting phosphate in the crystal structure are shown in blue and acidic residues comprising the acidic patch are in red. Residues conserved in HRDC #3's structural homologs for the HRDC #3 phosphate binding or acidic patch residues are also colored blue and red, respectively. (**E**) Phosphate ion present in the HRDC #3 crystal structure. The position of the phosphate ion and basic residues K805 and R806 are shown on the left side. To the right, a closer view of the surface of HRDC #3 and the phosphate ion surrounded by an omit map contoured at 5.0 σ. (**F**) Electrostatic surface diagram of HRDC #3 in orthogonal views [for positive (blue) and negative (red) surfaces].

all RecQ family members includes a Helicase, RecQ-conserved (RecQ-Ct) and HRDC domain (12). In *E. coli* RecQ (EcRecQ), the Helicase and RecQ-Ct domains combine to form a single structural domain that contains the conserved helicase motifs responsible for RecQ's enzymatic activities, a Zn^{2+} binding platform for conformational stability, and a winged-helix sub-domain for interactions with other proteins and DNA structures (13–17). The HRDC domain forms an independent helical bundle that is important for structure-specific DNA binding (12). DrRecQ contains each of these domains but has a total of three HRDC domains at its C-terminus (Figure 1A), a property shared only with the RecQ family members from *Neisseria gonorrhoeae* and *Neisseria meningitidis* (both non-radioresistant). Interestingly, each HRDC domain influences the biochemical functions of DrRecQ differently (18), raising the question of how the individual HRDC domains have achieved such specialization within the framework of their conserved structural fold.

The structures of isolated HRDC domains from EcRecQ, *S. cerevisiae* Sgs1 and Human Werner protein (WRN) all share a similar overall fold but exhibit contrasting functions (19–21). The EcRecQ and Sgs1 HRDC domains interact with DNA in a structure-specific manner and mutation or deletion of the HRDC can alter this specificity without serious consequences for ATP hydrolysis or helicase activities in the respective protein. In contrast, the isolated WRN HRDC does not interact with DNA *in vitro* and contains an extended loop rich

in acidic residues which has been proposed to mediate protein–protein interactions. The structures of *E. coli* RNaseD and *S. cerevisiae* Rrp6 further demonstrate HRDC domain specialization (22,23). These ribonuclease structures are of full-length proteins with HRDC domains and show the tenuous nature of the inter-domain interactions between their large, catalytic portions and HRDC domains. In both structures, a single acidic residue from the HRDC domain mediates contacts with the remainder of the protein. Mutation of this acidic residue in Rrp6 alters its structure-specific nuclease activity, attesting to the importance of such inter-domain contacts. The hypothesis suggested by these structures and *in vitro* biochemical data is that HRDC domains provide a malleable scaffold upon which to evolve specialized functions through changes to their surface-exposed residues. Therefore, an understanding of HRDC domain specialization provides critical details about how RecQ helicases can perform distinct, yet integrated functions in genome maintenance.

In this report, we describe the 1.1 Å resolution structure of the regulatory C-terminal-most HRDC domain of DrRecQ. This domain retains an overall fold similar to other HRDC domain structures, but features a concentrated patch of acidic residues and two sequential basic residues that ligand a phosphate ion in the crystal structure. We have examined the roles played by these structural features by creating individual alanine-substitution mutations in full-length DrRecQ and show that changes in these regions affect the enzyme's ability to bind DNA and unwind a partial duplex DNA substrate but not hydrolyze ATP in the presence of short ssDNA oligonucleotides. This is a surprising result given our previously observed increase in ssDNA-binding affinity and short ssDNA-dependent ATP hydrolysis upon removal of this domain from DrRecQ (18). We propose a model where the HRDC domain's acidic patch provides a surface for inter-domain interactions that function to direct DrRecQ binding to certain DNA structures as a mechanism of self-regulation.

MATERIALS AND METHODS

Cloning, expression and purification of DrRecQ constructs and variants

Expression plasmids pMK101 (encoding residues 1–824, DrRecQ) and pMK108 (residues 751–824, HRDC #3) were previously described (18). Alanine-substitution mutations in pMK101 were created according to the Quik Change mutagenesis protocol (Stratagene). The sequences of all plasmids were confirmed by DNA sequencing.

Plasmids were transformed into BL21(DE3) *E. coli* cells, grown at 37°C in Luria–Bertani medium supplemented with 50 μg/ml kanamycin to an $OD_{600} = 0.6$, and induced to overexpress protein by the addition of 1 mM isopropyl-β-D-thiogalactopyranoside for 4 h. Cells were harvested by centrifugation (10 min at 13 000*g*) and stored overnight at −80°C. Cell pellets were resuspended in lysis buffer (20 mM Tris, pH 8.0, 500 mM NaCl, 10% (v/v) glycerol, 1 mM 2-mercaptoethanol, 1 mM phenylmethylsulphonyl fluoride (PMSF), 100 mM dextrose and 15 mM imidazole), lyzed at 4°C by two passages through a French press, and clarified by centrifugation (30 min at 28 000*g*). All subsequent steps were carried out at 4°C. Soluble lysate was loaded onto a Ni^{2+}-NTA column and washed with 20 column volumes of lysis buffer. His-tagged protein was eluted with 3–6 column volumes of lysis buffer containing 250 mM imidazole and dialyzed overnight in lysis buffer lacking imidazole. Preparations of HRDC #3 were digested with thrombin to remove the His-tag (leaving a Gly-Ser-His sequence at the N-terminus), and passed over a second Ni^{2+}-NTA column to remove any uncleaved protein. The remaining protein was concentrated and purified through a Sephacryl S-100 size exclusion column (Pharmacia, Uppsala, Sweden) in 10 mM Tris, pH 8.0, 500 mM NaCl, 10% (v/v) glycerol, 1 mM 2-mercaptoethanol, 1 mM PMSF and 1 mM EDTA. HRDC #3 fractions were pooled, concentrated to 25 mg/ml, dialyzed against storage buffer (10 mM Tris, pH 8.0, 400 mM NaCl, 40% (v/v) glycerol, 1 mM 2-mercaptoethanol, 1 mM PMSF and 1 mM EDTA), and stored at −80°C. Selenomethionine-incorporated HRDC #3 was expressed as previously described (24), and purified identically to unsubstituted protein except that 1 mM Tris(s-carboxylethyl) phosphine hydrochloride was used instead of 2-mercaptoethanol in all buffers. For DrRecQ and variants, the Ni^{2+}-column eluent was dialyzed against lysis buffer lacking imidazole for 4 h, diluted 10-fold in dilution buffer (5 mM Tris, pH 8.0, 20% (v/v) glycerol, 1 mM 2-mercaptopethanol and 1 mM EDTA), and purified through a Q Sepharose Fast Flow ion exchange column (GE Healthcare, Uppsala, Sweden) equilibrated in QFF buffer (10 mM Tris, pH 8.0, 50 mM NaCl, 10% (v/v) glycerol, 1 mM 2-mercaptoethanol and 1 mM EDTA) with elution by gradually increasing the NaCl concentration to 1M. Fractions containing pure protein were pooled, concentrated to 10 mg/mL, dialyzed against storage buffer for 4 h, and stored at −80°C.

Crystallization of HRDC #3

HRDC #3 was dialyzed against 10 mM Tris, pH 8.0 and 50 mM NaCl at 4°C for 4 h. Crystals were grown by hanging-drop vapor diffusion at room temperature by suspending 1 μl of HRDC #3 (3 mg/ml) and 1 μl of mother liquor (1.8 M Na/K Phosphate, pH 4.0, 100 mM Hepes, pH 7.5) above 1 ml of mother liquor. Crystals measuring ~50 μm × ~300 μm × ~500 μm formed in one day and were transferred to a cryoprotectant solution (0.75 M Na/K Phosphate and 25% (v/v) ethylene glycol) prior to being flash-frozen in liquid nitrogen. Both native and selenomethionine-incorporated crystals diffracted to 1.1 Å resolution with unit cell dimensions a = b = 49.98 Å, c = 83.61 Å, and space group $P4_12_12$.

MAD phasing and model refinement

The structure of selenomethionine-incorporated HRDC #3 was solved to a resolution of 1.1 Å using multi-wavelength anomalous dispersion (MAD) phasing. The automated structure solution package Elves was used throughout data analysis and map construction (25). Data were indexed and scaled with MOSFLM (26) and SCALA

(27) and selenium sites were identified with SOLVE (28) and refined using MLPHARE (29). Interpretable electron density maps were created following solvent flattening using DM (30) and the initial model built using ARP/WARP (31) was adjusted manually using the program O (32). The model was further refined by multiple iterative rounds of refinement using REFMAC5 (33) and manual rebuilding.

Size exclusion chromatography

DrRecQ and its variants were dialyzed into 20 mM Tris, pH 8.0, 100 mM NaCl, 1 mM 2-mercaptoethanol, 1 mM $MgCl_2$ and 4% (v/v) glycerol. Proteins were resolved through a Superdex 200 gel filtration column (GE Healthcare) equilibrated in the same buffer and plotted as the absorbance of each sample as a function of its retention volume in the column. For reference, gel filtration standards (BioRad, Hercules, CA) were also run and the position of their elution peaks is indicated at the corresponding volume in the column.

DNA binding assays

Substrate preparation, measurement of DNA binding by fluorescence polarization (FP), and calculation of fraction bound were performed as previously described (18) for DrRecQ and each of its variants. Proteins were diluted in 20 mM Tris, pH 8.0, 100 mM NaCl, 1 mM 2-mercaptoethanol, 1 mM $MgCl_2$, 0.1 g/l of bovine serum albumin and 4% (v/v) glycerol and incubated with either a 0.2 nM fluoroscein-labeled 30-base ssDNA (o30, 5′-GCGTG GGTAATTGTGCTTCAATGGACTGAC-3′) or 1 nM fluoroscein-labeled 18 bp duplex DNA with a 12 base 3′-overhang (dup-3′) at room temperature in a total reaction volume of 100 µl. The dup-3′ substrate was created by heating and slow cooling an equimolar mixture of o30 and o18 (5′-AAGCACAATTACCCACGC-3′) to room temperature. The radio-labeled synthetic Holliday junction (HJ) substrate was prepared as previously described by heating and slow cooling a mixture of four complementary oligonucleotides (18). FP reactions were measured at 25°C using a Panvera Beacon 2000 FP system with 490 nm excitation and 535 nm emission wavelengths. The fraction of substrate bound in each sample was calculated by setting the anisotropy value of the fluorescein-labeled substrate in buffer alone (values were ~40 millianisotropy (mA) units) to zero and setting the anisotropy value at 10 µM protein concentration (values were ~220 mA) to 100% bound. Fluorescence intensity for all substrates and protein variants did not vary by >15% across the range of protein concentrations tested indicating that quantum yield differences between free DNA and protein-bound DNA did not significantly influence the anisotropy measurements. Each reaction was performed a minimum of three times and plotted as an average value with error bars corresponding to 1SD. Apparent K_d's were determined for each individual dataset and used to calculate their average, standard deviation and *P*-values using the MedCalc software program. Gel-based binding experiments were performed in buffer identical to FP reactions and contained 1 nM of the appropriate radio-labeled substrate. DrRecQ or its variants were added to the reaction mixture in a final volume of 20 µl and incubated at room temperature for 30 min. The bound products were resolved through a 6–8% native polyacrylamide gel, dried onto Whatman paper, and imaged using a Storm 820 Phosphorimager (Amersham Biosciences, Uppsala, Sweden).

DNA-dependent ATP hydrolysis assays

ATPase assays were performed as previously described (13). The ATPase activity of each DrRecQ variant was stimulated by the addition of 0.028–2800 nM (nucleotides) dT_{28}. For longer DNA substrates, assays were performed with 0.04–2800 nM (nucleotides) M13mp18 circular ssDNA (New England Biolabs, Ipswich, MA). Each reaction was performed a minimum of three times and plotted as an average value with error bars corresponding to 1SD.

Helicase assays

Reaction conditions were as described in (18). Briefly, T4 polynucleotide kinase was used to phosphorylate the 5′-end of o18 or oHolliday1 followed by annealing to their complimentary oligonucleotide(s) by heating and slow cooling to room temperature. The dup-3′ substrate created contains an 18-bp duplex region and a 12-base single-strand extension with a 3′-end and the synthetic HJ contains 20-bp duplex arms extending from a central, four-way junction. Serially diluted DrRecQ variants were incubated with 1 nM substrate for 30 min at room temperature in 20 mM Tris, pH 8.0, 50 mM NaCl, 1 mM 2-mercaptoethanol, 1 mM $MgCl_2$, 1 mM ATP, 0.1 g/l bovine serum albumin and 4% (v/v) glycerol. For assays testing ATP dependence, either 1 mM ADP or ATPγS were substituted for ATP in the reaction mixture. Reactions were quenched by the addition of 11% (v/v) glycerol, 0.29% SDS, and 5 ng of the unlabeled o18 or oHolliday1. Reaction products were resolved through 10–12% native polyacrylamide gel, dried onto Whatman paper, imaged using a Storm 820 Phosphorimager (Amersham Biosciences), and quantified using Image Quant 5.1 software. The percentage of DNA unwound is plotted as an average of at least three trials with error bars corresponding to 1SD from the mean.

RESULTS

Structure of *D. radiodurans* RecQ HRDC #3

The structure of HRDC #3 was solved to 1.1 Å resolution, making it the highest resolution HRDC domain structure determined to date. Residues 751–824 of DrRecQ were built into well-defined electron density maps (Figure 1B) generated using MAD phasing and solvent flattening. The final structure was refined with good stereochemical and structural statistics (Table 1).

The overall HRDC #3 structure adopts a globular fold comprising five α-helices connected by short loop regions similar to those of other HRDC domain structures (Figure 1C). HRDC #3 begins with a long, N-terminal

Table 1. Data collection, phasing and refinement statistics

	Peak λ	Low energy λ
Data collection		
Wavelength (Å)	0.9797	0.9999
Resolution range (Å)	83.6–1.1 (1.16–1.10)	83.6–1.1 (1.16–1.10)
Completeness (%)	96.6 (78.7)	94.0 (64.8)
Total reflections	275,102	261,308
Unique reflections	42,318	41,193
$<I/\sigma I>$	13.8 (1.8)	16.9 (2.4)
R_{sym}[a] (%)	6.7 (41.9)	5.9 (27.1)
Phasing		
Figure of merit	0.376; 0.613 after solvent flattening	
Refinement		
Resolution (Å)	20–1.1	
R_{work}/R_{free}[b] (%)	17.7/19.4	
Rms deviations		
Bonds (Å)	0.010	
Angles (°)	1.23	
Ramachandran plot (%)		
Most favored	95.6	
Allowed	4.4	
Generously allowed	0.0	
Disallowed	0.0	

[a] $R_{sym} = \Sigma\Sigma_j|I_j - <I>|/\Sigma I_j$ where I_j is the intensity measurement for reflection j and $<I>$ is the mean intensity for multiply recorded reflections.
[b] $R_{work,\ free} = \Sigma||F_{obs}| - |F_{calc}||/|F_{obs}|$, where the working and free R factors are calculated using the working and free reflection sets, respectively. The free R reflections (5% of the total) were held aside throughout refinement.

α-helix (α1) that is separated from the short α2 by a hydrophobic loop. This region is flanked by the compact helix-loop-helix stretch of α3 and α4 that positions α5 into a close, anti-parallel orientation with α1. A search for structural homologs of HRDC #3 using the DALI search engine (34) revealed the strongest structural similarities (Z-score > 7.0) were with the HRDC domains of *E. coli* RNaseD [root mean square deviation (r.m.s.d.): 1.2 Å for 74 Cα atoms], EcRecQ (r.m.s.d.: 1.1 Å for 69 C_α atoms), Sgs1 (r.m.s.d.: 2.0 Å for 72 C_α atoms), Rrp6 (rmsd: 1.7 Å for 74 C_α atoms) and human WRN (rmsd: 1.4 Å for 74 C_α atoms). A sequence alignment of these homologs demonstrates the low amount of sequence conservation with HRDC #3 despite the retention of an HRDC domain fold in these proteins (Figure 1D).

Two distinguishing features within HRDC #3 include an expansion of ionic interactions among separate helices and proline residues that restrict loop orientation. An example of the ionic features is a salt bridge formed between α1 and α5 through the interaction of E768 and R813 side chains. These interacting partners are separated by 45 residues in primary structure, but folding of HRDC #3 allows their close association (2.9 Å). Among HRDC #3's close structural homologs, E768 is found in RNaseD and EcRecQ, but the interaction with α5 is not formed in these HRDC domains. For R813, the Sgs1 HRDC domain has an analogous arginine residue that was implicated in DNA binding by NMR chemical shift experiments (21). Therefore, the usage of this arginine to form an ionic interaction in HRDC #3 could limit its ability to interact with DNA, consistent with our previous observation that isolated HRDC #3 has a very low affinity for DNA (18,21). In contrast to this variable inter-helix bridge, a prominent polar interaction that occurs between R762 and N779 is conserved across HRDC #3's closest structural homologs. The proximity of these residues results from the hydrophobic loop connecting α1 to α2 that folds the structure back onto itself. Due to the high relative B-factors of this exposed hydrophobic region, this ionic interaction may be favored as a means to stabilize the HRDC framework. Mutation of the arginine at this position in EcRecQ HRDC results in a greater than 10-fold reduction in ssDNA binding, suggesting this may be a weak interaction in those HRDC domains that bind nucleic acids strongly (19). The last notable interaction occurs between R791 and N819 connecting the loop following α3 to α4. This interaction is not seen in HRDC #3's structural homologs, although the loop contains a proline (P790) that is strictly conserved across these different HRDC domains (Figure 1D). In each structure, this proline residue kinks the loop inwards; inverting the surrounding residues to project their side chains outwards. In HRDC #3, this restricts the loop conformation, allowing the inter-helix bridge to form between R791 and N819. A similar interaction is seen in the WRN HRDC domain structure although the arginine residue in its loop is positioned to interact with α1 instead of α4 as a proposed means to stabilize its elongated N-terminal α1 (20). HRDC #3 also appears to use a proline (P800) to restrict the loop conformation between α4 and α5 containing the conserved hydrophobic residues V799 and L802. While the latter residues are conserved among other HRDC domains, the proline is not and may further contribute to HRDC #3's stability by locking these hydrophobic residues into the interior of the domain.

Phosphate binding in the HRDC 3 crystal structure

Electron density maps of HRDC #3 displayed a well-ordered, electron-dense ligand bound near the C-terminus of α1 (Figure 1E). The tetrahedral shape of the density suggested that a phosphate ion from the crystallization buffer was bound to HRDC #3 in the crystal lattice. The phosphate ion bridges HRDC #3 symmetry mates within the lattice, with residues K805 and R806 of one molecule and K767 of the adjacent symmetry mate liganding the ion. Phosphate association at this position suggested that these residues could be involved in forming contacts to the phosphate backbone of DNA, which we tested below. Although the isolated HRDC #3 binds DNA with low affinity ($K_{d,app}$ > 10 μM) (18), it is possible that in the context of the full-length protein this region is capable of contacting DNA. Evidence for such an interaction is provided by observations made in RNaseD, EcRecQ and Sgs1 HRDC domains. The crystal structure of RNaseD contains a sulfate ion in a similar position to the HRDC #3 phosphate, and it is also bound by an arginine residue that is located in a similar region to R806 (23). In Sgs1, the analogous lysine–arginine pair display large NMR

chemical shifts differences upon the addition of DNA, consistent with DNA binding to this surface (21). Furthermore, of all the residues in the Sgs1 HRDC domain that responds to the addition of DNA in this manner, only the lysine residue is conserved with the WRN and Bloom's protein (BLM) HRDC domains. Interestingly, this lysine is required in BLM for efficient dissolution of synthetic double HJs (35). In the isolated EcRecQ HRDC domain, mutation of K587 corresponding to HRDC #3 R806 results in a 10-fold decrease in ssDNA-binding affinity by electrophoretic mobility shift assay (36). Thus, comparison of HRDC #3's structural features with its homologs suggests it may play a role in DNA binding in DrRecQ.

The HRDC #3 domain contains a prominent acidic patch

The most striking feature unique to HRDC #3 is the concentration of acidic residues on a surface comprising the terminal portions of α1 and α5 (Figure 1F). Several acidic residues including D753, E756, E760, E764 and D816 contribute to the domain's large electronegative surface. These residues are not conserved among other HRDC domains, including HRDC #1 and #2 in DrRecQ (Figure 1D). Furthermore, the calculated isoelectric point (pI) of HRDC #3 is 4.6, another property that contrasts sharply with HRDC #1 (pI = 7.4) and HRDC #2 (pI = 8.8). The HRDC #3 structure shows that many of these acidic residues are clustered on one face of the domain (Figure 1F), suggesting that the acidic character of HRDC #3 could be tailored for a specific function in DrRecQ. This observation raised the possibility that the acidic patch of HRDC #3 could be a site for inter-domain interactions that are similar to HRDC domains in RNaseD and Rrp6 (22,23). Such an interface between HRDC #3 and the rest of DrRecQ could help explain our earlier observations that the presence of this domain reduces the protein's ability to bind ssDNA and hydrolyze ATP in a DNA-dependent manner (18).

DNA binding by DrRecQ variants

To test whether residues involved in phosphate binding or formation of the acidic patch affect the function of DrRecQ, we created single alanine-substitution mutations altering these regions in the full-length protein (Figure 2A). Purified DrRecQ variants were tested *in vitro* for their ability to bind DNA by observing DrRecQ-dependent changes in the fluorescence anisotropy of a fluoroscein-labeled ssDNA or dup-3′ DNA. Gel-shift analysis was used to test binding to synthetic HJ DNA because we had previously observed multiple binding events by DrRecQ variants using fluorescence anisotropy that made interpretation of the results difficult (18). Our hypothesis was that basic residues that bound phosphate in the HRDC #3 crystal structure could play roles in DNA binding and that their mutation to alanine could result in decreased DNA binding affinity. DrRecQ bound ssDNA with a $K_{d,app}$ of 1.3 ± 0.5 nM (Figure 2B, Table 2). Substitution of alanine at either K805 or R806 resulted in modest 2-fold binding defects ($K_{d,app}$ of 2.5 ± 0.6 nM and 2.7 ± 0.2 nM for each mutant, respectively) although only the defect in R806A ssDNA binding appeared to be statistically significant, with a *P*-value of 0.0078 (Figure 2B, Table 2). Likewise, the $K_{d,app}$ for binding to the dup-3′ substrate was weakened 2-fold or less from 143.6 ± 23.4 nM for DrRecQ to 279.0 ± 17.7 nM for K805A and 177.9 ± 98.3 nM for R806A (Figure 2C, Table 2). Only the K805A mutant showed a statistically significant difference from WT on the dup-3′ substrate ($P = 0.0013$). We also observed modestly reduced HJ binding affinity for the K805A variant relative to DrRecQ, suggesting mutation of this residue compromises stable association with HJ DNA (Figure 3). These results indicate that phosphate binding residues in HRDC #3 could play a minor role in DNA binding, although the relatively modest binding defects of their variants suggest the remainder of DrRecQ provides the major DNA binding surfaces on the enzyme.

We next determined the effect of mutations in the acidic patch of HRDC #3 to test our hypothesis that these residues help form an inter-domain interface that is important for enzyme function. If such inter-domain interactions position HRDC #3 properly, we hypothesized that mutations in this region could alter DrRecQ DNA binding. We observed a strong defect in binding to both ssDNA and dup-3′ following alanine-substitution at D816. The D816A mutant had a $K_{d,app}$ of 6.9 ± 0.7 nM for ssDNA, an approximate 5-fold decrease in affinity relative to wild-type (WT) DrRecQ (Figure 2D, Table 2). This variant also had a 10-fold decrease in dup-3′ binding, with a $K_{d,app}$ of 1282.2 ± 95.7 nM (Figure 2E, Table 2) and a ~5-fold decrease in ability to shift HJ DNA (Figure 3). Mutations in other residues comprising the acidic patch did not have a significant effect on binding to ssDNA or HJ DNA (Table 2, Supplementary Figure 1A, Supplementary Figure 2), although we did observe a 2–4-fold reduction in their affinity for the dup-3′ substrate (Supplementary Figure 1B, Table 2). The defects observed for these variants are not likely to be due to differences in oligomeric state or aggregation of the proteins since DrRecQ, R806A and D816A at concentrations >100 μM all displayed equal mobility by analytical gel filtration in buffer conditions identical to our DNA binding reactions (Supplementary Figure 3). In addition, gel-shift assays testing binding of DrRecQ and D816A to ssDNA and dup-3′ show these proteins do not have observable differences in oligomeric state when bound to DNA and are consistent with a single-site binding model (Supplementary Figure 1C and D). The DNA binding defects of the acidic patch mutants are consistent with the hypothesis that they make interactions important for the proper function of DrRecQ. In particular, D816 appears to be important for proper DrRecQ function. Since each of these mutations resulted in a more pronounced dup-3′ binding defect than ssDNA or HJ binding, it is possible that interactions formed by these residues in HRDC #3 help impart substrate specificity to DrRecQ.

DNA-dependent ATP hydrolysis by DrRecQ variants

To examine the enzymatic activity of the DrRecQ variants, we first tested their DNA-dependent ATP hydrolysis

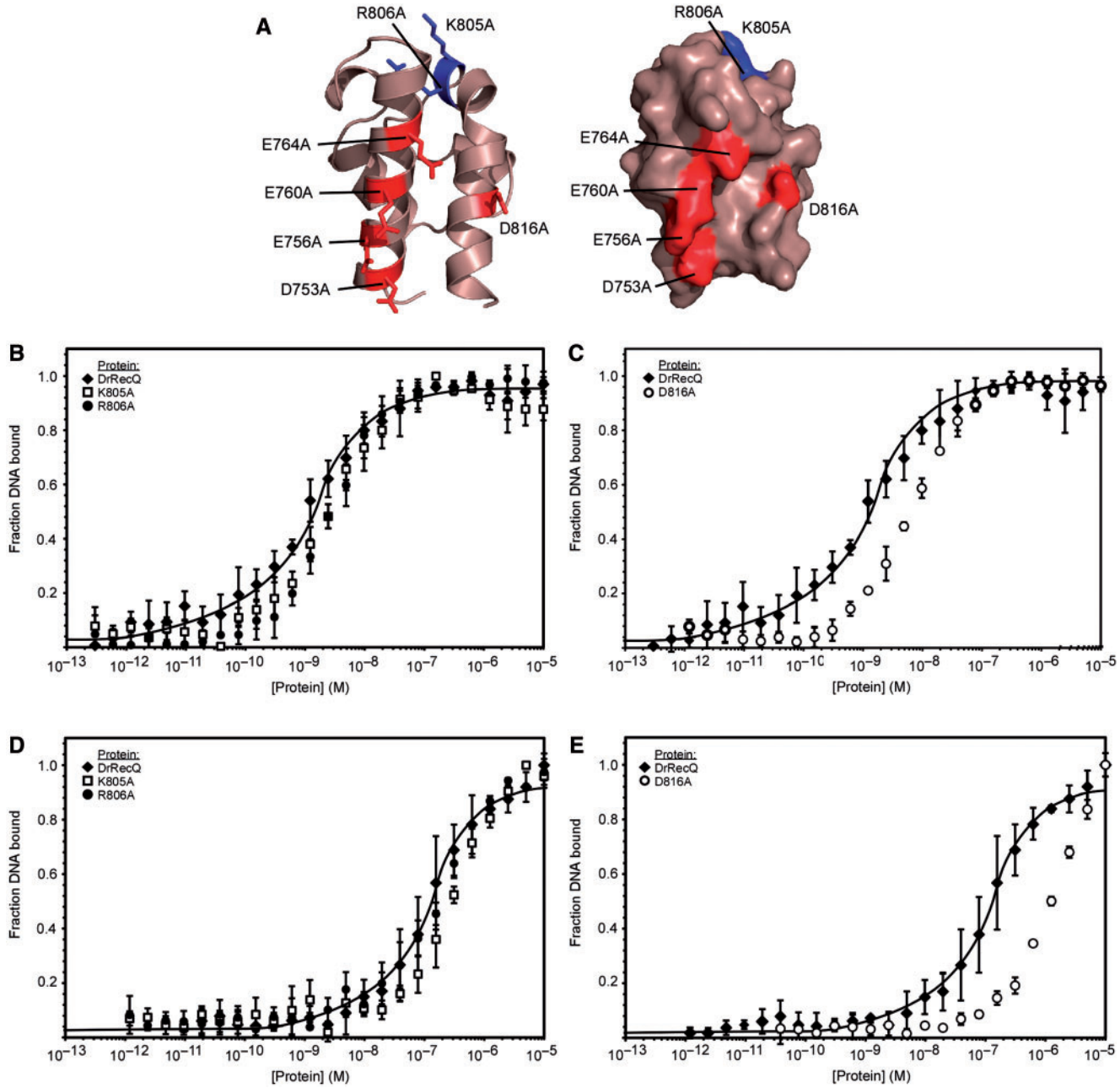

Figure 2. DrRecQ variants have reduced affinity for ssDNA and dup-3′ DNA. (**A**) The positions of alanine-substitution mutations are indicated on ribbons (left) and surface (right) representations of the HRDC #3 structure. Residues in close proximity to a phosphate ion in the crystal structure are shown in blue, with those comprising the acidic patch in red. (**B**–**E**) Fraction of DNA bound with either ssDNA (B and D) or dup-3′ (C and E) by DrRecQ variants with mutations in the phosphate binding site (B and C) or D816 in the acidic patch (D and E). DrRecQ (closed diamonds), K805A (open squares), R805A (closed circles) and D816A (open circles). A trend line for DrRecQ is shown in each plot for reference.

activities (Figure 4). We expected that if any of the mutated residues contributed to the efficient binding of ssDNA or conformational changes associated with the active enzyme that their rate of ATP hydrolysis would change accordingly. Each of the DrRecQ variants in the phosphate-binding site (Figure 4A) and the acidic patch variant D816A (Figure 4B) catalyzed ATP hydrolysis at similar maximal rates and were activated by dT_{28} in a manner that was indistinguishable from WT DrRecQ. Likewise, we observed no differences between DrRecQ and the other acidic patch mutants in their ability to hydrolyze ATP in this assay (Supplementary Figure 4A). These results indicate that the variants are competent to recognize ssDNA, and hydrolyze ATP despite the observation that several (K805A, R806A and D816A) had defects in ssDNA binding. These results may be specific to shorter oligonucleotides, since performing the assay in the presence of M13mp18 circular ssDNA showed that the D816A had a greater activity than DrRecQ and was not saturated at higher DNA concentrations, suggesting there may be differences in how this variant binds and translocates along DNA (Supplementary Figure 4B).

The increase in D816A ATPase activity on long ssDNA is similar to the change observed upon removal of HRDC #3 from DrRecQ on the short dT_{28} substrate (18).

Helicase activity of DrRecQ variants

Finally, we tested the ability of the DrRecQ variants to unwind synthetic dup-3′ and HJ DNA substrates. These are two of the preferred substrates for DrRecQ unwinding *in vitro* and could be structures targeted by the enzyme *in vivo* (18). Since helicase activity integrates both DNA binding and ATP hydrolysis, we were interested to see if any of our DrRecQ variants would unwind DNA differentially. DrRecQ unwound half of the dup-3′ substrate at a concentration of ~13 pM in an ATP-dependent manner (Figure 5A, Supplementary Figure 5A and B). Figure 5A also shows that R806A, but not K805A, exhibits a defect (~2.5-fold) in its ability unwind the dup-3′ substrate, suggesting this residue could play a minor role in DNA unwinding. These variants were as proficient as DrRecQ in unwinding HJ DNA (Supplementary Figure 6). The D816A variant showed an apparent increase in its ability to unwind dup-3′ DNA at low concentrations (Figure 5B) that we attribute to normalization of the data and did not observe for other acidic patch variants (Supplementary Figure 7A). Interestingly, when we repeated the assay at salt concentrations identical to the DNA-binding assays, the D816A variant had a decreased ability to unwind dup-3′ ~50-fold (Supplementary Figure 7B). At higher

Table 2. Statistical comparison of DrRecQ variant UNA binding

Protein	$K_{d,app}$[a,c]	SD[a]	*P*-value[a,d]	$K_{d,app}$[b,c]	SD[b]	*P*-value[b,d]
DrRecQ	1.3	0.5	–	143.6	23.4	–
D753A	1.6	0.1	0.3134	408.6	23.6	.0002
E756A	1.2	0.2	0.6716	205.0	21.6	.0289
E760A	0.8	0.2	0.1372	278.7	38.2	.0064
E764A	1.0	0.2	0.3873	319.1	17.7	.0005
K805A	2.5	0.6	0.0586	279.0	17.7	.0013
R806A	2.7	0.2	0.0078	177.9	98.3	.5888
D816A	6.9	0.7	0.0004	1282.2	95.7	<.0001

[a]ssDNA binding (in nM).
[b]dup-3′ binding (in nM).
[c]Mean $\kappa_{d,app}$ of three independent trials.
[d]Calculated using independent samples *t*-test (MedCalc).

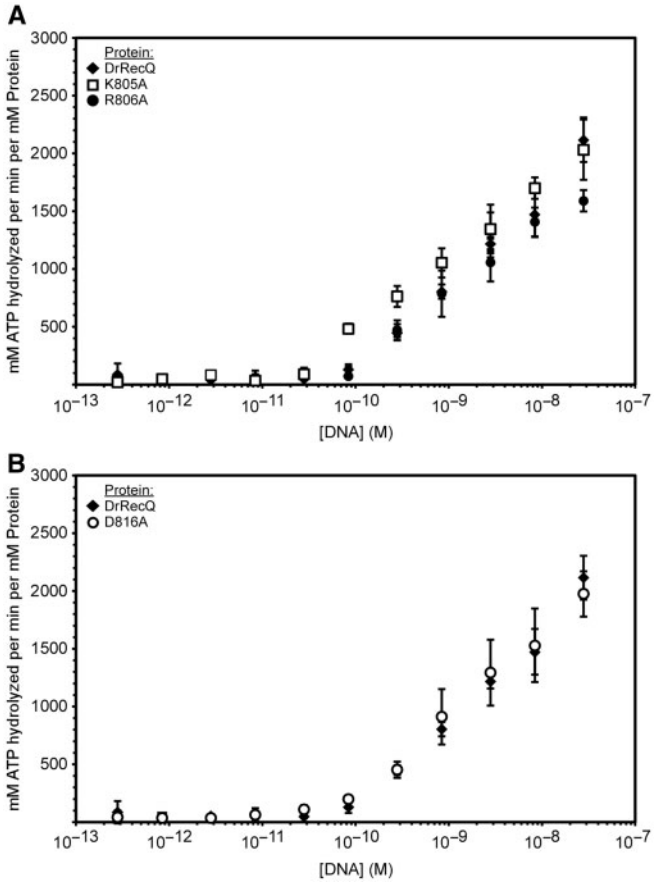

Figure 4. Variants in DrRecQ HRDC #3 do not affect DNA-dependent ATP hydrolysis with short ssDNA. The rate of ATP hydrolysis for DrRecQ and (**A**) phosphate-binding site variants K805A and R806A and (**B**) acidic patch variant D816A are plotted as a function of ssDNA concentration (in nucleotides). DrRecQ (closed diamonds), K805A (open squares), R806A (closed circles) and D816A (open circles).

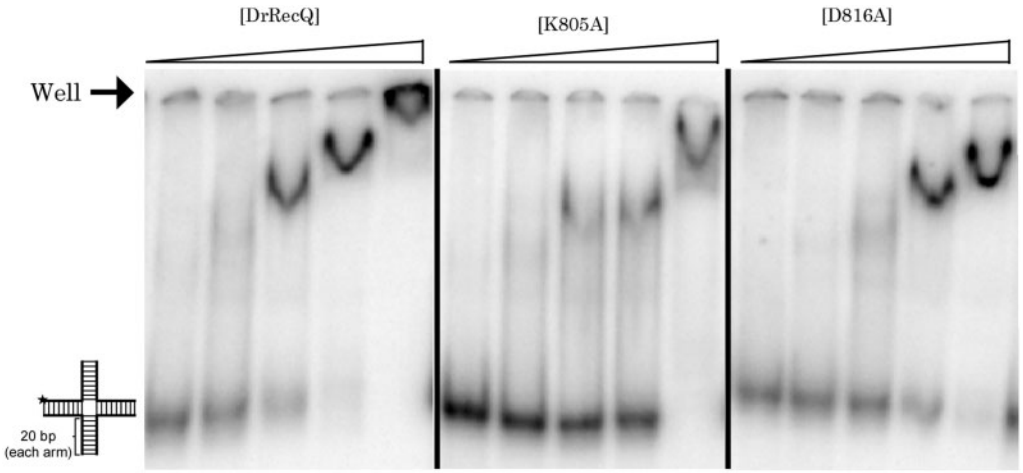

Figure 3. The D816A and K805A mutants have defects in synthetic HJ binding. Increasing concentrations (1.6 nM, 8 nM, 40 nM, 200 nM, 1 μM) of DrRecQ, K805A and D816A added to a synthetic HJ substrate. The position of the wells and the unbound substrate is indicated on the left side.

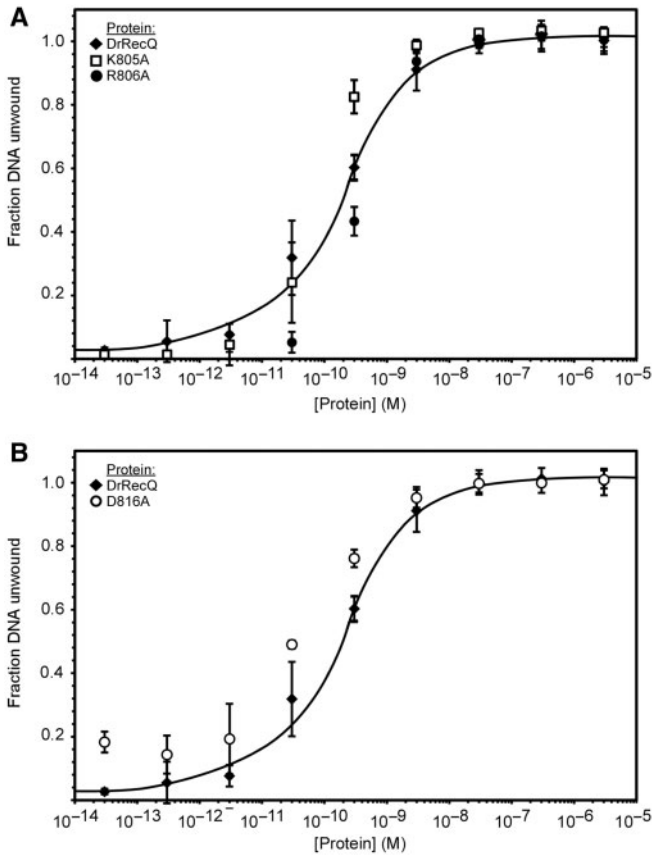

Figure 5. DrRecQ variants have differing helicase activities. The fraction of dup-3′ DNA unwound by DrRecQ, (**A**) phosphate binding site variants K805A and R806A, and (**B**) acidic patch variant D816A are plotted as a function of protein concentration (0.3 pM to 300 nM). DrRecQ (closed diamonds), K805A (open squares), R806A (closed circles) and D816A (open circles). A trend line for DrRecQ is shown for reference.

salt concentrations, DrRecQ unwound half the dup-3′ DNA at 80 pM while the D816A variant required 240 pM for 50% unwinding. This is consistent with its defect in dup-3′ binding by FP and gel-shift assay at these salt concentrations. In contrast, DrRecQ's helicase activity was only reduced 6-fold at higher salt concentrations demonstrating that the D816A mutant is particularly sensitive to the ionic strength of the reaction conditions. All of the acidic patch variants unwound HJ DNA as well as DrRecQ (Supplementary Figure 6). Therefore, the binding defect we observed for the D816A variant on HJ DNA by gel shift does not seem to affect its unwinding activity on this substrate.

DISCUSSION

Determining how the conserved domains of RecQ family members are specialized in their distinct functions is critical to our understanding of their biological roles. In this report, we describe the high-resolution structure of the C-terminal-most HRDC domain of *D. radiodurans* RecQ. This domain adopts a similar overall fold to other HRDC domains but contains a number of additional intra-domain interactions and proline residues that contribute to its compact tertiary structure. We observed a well-ordered phosphate ion bound between HRDC #3 symmetry mates contacted by basic residues homologous to those involved in DNA binding in EcRecQ, Sgs1 and BLM. Mutation of these residues to alanine in DrRecQ modestly decreased the enzyme's ability to bind DNA but had no effect on short-ssDNA-dependent ATPase activity or, in the case of R806A, to unwind a dup-3′ substrate. These results demonstrate a possible minor role for HRDC #3 in DNA binding, although it is clear that the major DNA-binding and catalytic functions lay elsewhere in the protein. HRDC #3 also features a prominent acidic patch that arises from the clustering of five acidic residues near its N- and C-termini. Mutation of D816 leads to defect in binding to several DNA substrates, whereas individual mutation in other acidic patch residues results in decreased DNA binding only to a dup-3′ substrate. Each of the acidic patch variants was comparable to WT DrRecQ in ATP hydrolysis on short ssDNA and DNA unwinding assays with the exception of the D816A variant, which showed a marked salt-sensitivity to its dup-3′ DNA unwinding activity. Together, these data suggest that the acidic patch (D816 in particular) could play a role in properly positioning HRDC #3 for binding and unwinding certain DNA structures. Such acidic HRDC interfaces have been observed previously in the RNaseD and Rrp6 structures, each of which relies upon a single acidic residue to dock the HRDC domain against the catalytic domain of the protein (22,23), as is described in greater detail subsequently. Collectively, these structural features demonstrate how HRDC domains have diverged and support the hypothesis that electrostatic differences modulate the activities of HRDC domains.

A functional role in DNA binding by HRDC domains is conserved in enzymes acting on nucleic acids

Retention and proliferation of HRDC domains in enzymes found throughout the kingdoms of life attests to their utility as key components in nucleic acid metabolism. These domains appear to provide structure specificity to RecQ DNA binding in a way that could help differentiate their functions in organisms that have several RecQ homologs. Structural descriptions of HRDC domains have provided a much-needed physical explanation for the *in vitro* and *in vivo* data indicating their importance to RecQ family members, ribonucleases and polymerases. From these data, a model emerges wherein cells have taken advantage of the functional plasticity of HRDC domains to evolve distinctive roles for the domains in different protein contexts.

The high-resolution structures of several HRDC domains have revealed how clustered electrostatic features on the domain surface can be important for the domain's function. Solution of the Sgs1 HRDC domain structure first described its use of a basic patch to interact with DNA and showed by homology modeling the lack of conservation of this surface in BLM and WRN HRDC domains (21). The recent crystal structure of the WRN HRDC domain confirmed this finding by revealing a large

cluster of acidic and hydrophobic residues as one of its distinctive features (20). Homologs in bacteria such as the RNaseD and EcRecQ HRDC domains feature their own patterns of acidic and basic residues. In the latter, several of these basic residues form a major ssDNA binding site on EcRecQ (19). In addition, structures of the HRDC domains from Rrp6 and sub-complexes of *S. cerevisiae* RNA polymerase III have provided examples of specializing surface charges that form interfaces with other parts of the protein (22,37).

The structures of HRDC domains from Sgs1, EcRecQ and DrRecQ have each led to further investigation of conserved basic residues near the N-terminus of α5. The K805A and R806A mutations in DrRecQ exhibit modest defects in binding to ssDNA, dup-3′ and HJ substrates (Figure 2B and C, Supplementary Figure 2). In the case of DrRecQ HRDC #3, R806A also seems to play a role in DNA unwinding. An analogous lysine residue to K805A in Sgs1 undergoes a large chemical shift by NMR upon the addition of partially duplex DNA (21), and in BLM is required for efficient dissolution of synthetic double HJ (35). Moreover, mutation of the analogous residue in EcRecQ (K587) results in a 10-fold reduction in ssDNA binding affinity. Therefore, it appears that this region of the HRDC fold has retained some involvement in DNA binding in DrRecQ despite specialization of other parts of the domain.

Possible functions of the HRDC #3 acidic patch

We have previously demonstrated that truncation of the protein's C-terminal HRDC domains alters its biochemical activities and show here the structure of HRDC #3 has a prominent acidic patch that is not conserved in any of its closest structural homologs. There is compelling evidence for inter-domain interactions involving HRDC domains wherein acidic residues from the HRDC element form critical ionic interfaces with the catalytic portions of the proteins. Two examples come from the RNaseD and Rrp6 proteins. The HRDC domains of these related ribonucleases associate with the rest of the molecule primarily through an interaction comprising a single acidic residue from the HRDC domain. Mutation of the acidic residue or its interaction partners forming the inter-domain interactions in Rrp6 results in an inability to properly process the 3′-end of only a subset of its target RNAs without affecting its catalytic activity (22,23). We observe a similar outcome upon mutation of residues in the HRDC #3 acidic patch, where ssDNA and HJ binding is unaffected by most mutations but binding to a dup-3′ DNA is reduced. In addition, the inter-domain interactions in RNaseD bury very modest surface areas for each of its HRDC domains (270 $Å^2$ and 500 $Å^2$), respectively (23). Both HRDC #3 and its closest structural homolog, RNaseD's N-terminal HRDC domain, are tethered to their neighboring domains through an extended linker rich in proline and glycine residues. These observations attest to the mobility of HRDC domains that could allow for reorientation following substrate recognition or catalysis in DrRecQ.

Based upon the results described in this work and the compelling similarities with earlier studies of HRDC domains in other systems, we propose that the acidic patch on HRDC #3 could function by forming an interaction surface that is complementary to a basic site on DrRecQ. In this model, an ionic interface buries HRDC #3's acidic patch against the remaining portion of DrRecQ; such an interaction could orient HRDC #3 so that it inhibits DNA binding by the helicase domain to attenuate ATP hydrolysis and subsequent unwinding. Indeed, truncation of HRDC #3 from DrRecQ increases its affinity for ssDNA and its rate of ssDNA-dependent ATP hydrolysis (18). When positioning of HRDC #3 is disrupted (e.g. by mutation of D816), the domain loses some of its ability to regulate DrRecQ function. Evidence for this comes from observations that mutation of D816 increases ATPase activity of DrRecQ on long DNA substrates [similar to removing the domain entirely on short ssDNA (18)] and sensitizes DrRecQ to elevated salt concentrations in helicase assays. A mechanism of self-regulation such as this may limit the processivity of DrRecQ or alter the DNA structures upon which it acts. Such effects could be favorable in *D. radiodurans*, which is believed to have been selected to tolerate desiccation and fluctuating intracellular conditions that damage DNA and lead to chronic accumulation of aberrant DNA structures (38).

The structure of HRDC #3 presented here highlights several features that are unique to this domain and suggests how its regulatory function is manifest. Future experiments designed to test association among the domains of DrRecQ will be important for resolving how it has expanded use of HRDC domains to modulate its function in *D. radiodurans*. It will be intriguing to examine HRDC function in other model systems as well to determine how multiple HRDC domains affect the cellular functions of RecQ family members beyond *D. radiodurans*.

SUPPLEMENTARY DATA

Supplementary Data are available at NAR Online.

ACKNOWLEDGEMENTS

We thank Dr James Holton at the ALS in Berkeley, CA for data collection, Nicholas George for expertise in protein purification and other members of the Keck Lab for critical reading of the article. This work was funded by National Institutes of Health (GM067085, J.K.) (PDBID: 2RHF) M.P.K. was supported in part by a NIH training grant in Molecular Biophysics and is a Cremer Scholar. Funding to pay the Open Access publication charges for this article is provided by the NIH and the University of Wisconsin, Madison Libraries.

Conflict of interest statement. None declared.

REFERENCES

1. Bachrati,C.Z. and Hickson,I.D. (2003) RecQ helicases: suppressors of tumorigenesis and premature aging. *Biochem. J.*, **374**, 577–606.

2. Ellis,N.A., Groden,J., Ye,T.Z., Straughen,J., Lennon,D.J., Ciocci,S., Proytcheva,M. and German,J. (1995) The Bloom's syndrome gene product is homologous to RecQ helicases. *Cell*, **83**, 655–666.
3. Kitao,S., Shimamoto,A., Goto,M., Miller,R.W., Smithson,W.A., Lindor,N.M. and Furuichi,Y. (1999) Mutations in RECQL4 cause a subset of cases of Rothmund–Thomson syndrome. *Nat. Genet.*, **22**, 82–84.
4. Yu,C.E., Oshima,J., Fu,Y.H., Wijsman,E.M., Hisama,F., Alisch,R., Matthews,S., Nakura,J., Miki,T., Ouais,S. *et al.* (1996) Positional cloning of the Werner's syndrome gene. *Science*, **272**, 258–262.
5. Bennett,R.J. and Keck,J.L. (2004) Structure and function of RecQ DNA helicases. *Crit. Rev. Biochem. Mol. Biol.*, **39**, 79–97.
6. Cox,M.M. and Battista,J.R. (2005) Deinococcus radiodurans – the consummate survivor. *Nat. Rev. Microbiol.*, **3**, 882–892.
7. White,O., Eisen,J.A., Heidelberg,J.F., Hickey,E.K., Peterson,J.D., Dodson,R.J., Haft,D.H., Gwinn,M.L., Nelson,W.C., Richardson,D.L. *et al.* (1999) Genome sequence of the radioresistant bacterium Deinococcus radiodurans R1. *Science*, **286**, 1571–1577.
8. Horii,Z. and Clark,A.J. (1973) Genetic analysis of the recF pathway to genetic recombination in Escherichia coli K12: isolation and characterization of mutants. *J. Mol. Biol.*, **80**, 327–344.
9. Hegde,S.P., Qin,M.H., Li,X.H., Atkinson,M.A., Clark,A.J., Rajagopalan,M. and Madiraju,M.V. (1996) Interactions of RecF protein with RecO, RecR, and single-stranded DNA binding proteins reveal roles for the RecF-RecO-RecR complex in DNA repair and recombination. *Proc. Natl Acad. Sci. USA*, **93**, 14468–14473.
10. Morimatsu,K. and Kowalczykowski,S.C. (2003) RecFOR proteins load RecA protein onto gapped DNA to accelerate DNA strand exchange: a universal step of recombinational repair. *Mol. Cell*, **11**, 1337–1347.
11. Ivancic-Bace,I., Salaj-Smic,E. and Brcic-Kostic,K. (2005) Effects of recJ, recQ, and recFOR mutations on recombination in nuclease-deficient recB recD double mutants of Escherichia coli. *J. Bacteriol.*, **187**, 1350–1356.
12. Morozov,V., Mushegian,A.R., Koonin,E.V. and Bork,P. (1997) A putative nucleic acid-binding domain in Bloom's and Werner's syndrome helicases. *Trends Biochem. Sci.*, **22**, 417–418.
13. Bernstein,D.A. and Keck,J.L. (2003) Domain mapping of Escherichia coli RecQ defines the roles of conserved N- and C-terminal regions in the RecQ family. *Nucleic Acids Res.*, **31**, 2778–2785.
14. Bernstein,D.A., Zittel,M.C. and Keck,J.L. (2003) High-resolution structure of the E.coli RecQ helicase catalytic core. *Embo. J.*, **22**, 4910–4921.
15. Hu,J.S., Feng,H., Zeng,W., Lin,G.X. and Xi,X.G. (2005) Solution structure of a multifunctional DNA- and protein-binding motif of human Werner syndrome protein. *Proc. Natl Acad. Sci. USA*, **102**, 18379–18384.
16. Liu,J.L., Rigolet,P., Dou,S.X., Wang,P.Y. and Xi,X.G. (2004) The zinc finger motif of Escherichia coli RecQ is implicated in both DNA binding and protein folding. *J. Biol. Chem.*, **279**, 42794–42802.
17. Shereda,R.D., Bernstein,D.A. and Keck,J.L. (2007) A central role for SSB in Escherichia coli RecQ DNA helicase function. *J. Biol. Chem.*, **282**, 19247–19258.
18. Killoran,M.P. and Keck,J.L. (2006) Three HRDC domains differentially modulate deinococcus radiodurans RecQ DNA helicase biochemical activity. *J. Biol. Chem.*, **281**, 12849–12857.
19. Bernstein,D.A. and Keck,J.L. (2005) Conferring substrate specificity to DNA helicases: role of the RecQ HRDC domain. *Structure*, **13**, 1173–1182.
20. Kitano,K., Yoshihara,N. and Hakoshima,T. (2007) Crystal structure of the HRDC domain of human Werner syndrome protein, WRN. *J. Biol. Chem.*, **282**, 2717–2728.
21. Liu,Z., Macias,M.J., Bottomley,M.J., Stier,G., Linge,J.P., Nilges,M., Bork,P. and Sattler,M. (1999) The three-dimensional structure of the HRDC domain and implications for the Werner and Bloom syndrome proteins. *Structure*, **7**, 1557–1566.
22. Midtgaard,S.F., Assenholt,J., Jonstrup,A.T., Van,L.B., Jensen,T.H. and Brodersen,D.E. (2006) Structure of the nuclear exosome component Rrp6p reveals an interplay between the active site and the HRDC domain. *Proc. Natl Acad. Sci. USA*, **103**, 11898–11903.
23. Zuo,Y., Wang,Y. and Malhotra,A. (2005) Crystal structure of Escherichia coli RNase D, an exoribonuclease involved in structured RNA processing. *Structure*, **13**, 973–984.
24. Van Duyne,G.D., Standaert,R.F., Karplus,P.A., Schreiber,S.L. and Clardy,J. (1993) Atomic structures of the human immunophilin FKBP-12 complexes with FK506 and rapamycin. *J. Mol. Biol.*, **229**, 105–124.
25. Holton,J. and Alber,T. (2004) Automated protein crystal structure determination using ELVES. *Proc. Natl Acad. Sci. USA*, **101**, 1537–1542.
26. Leslie,A.G.W. (1992) *Newsletter on Protein Crystallography No.26. Daresbury Laboratory*, Warrington, UK.
27. Kabsch,W. (1988) Evaluation of single-crystal X-ray diffraction from a position sensitive detector. *J. Appl. Crystallogr*, **21**, 916–924.
28. Terwilliger,T.C. and Berendzen,J. (1999) Automated MAD and MIR structure solution. *Acta Crystallogr. D Biol. Crystallogr.*, **55**, 849–861.
29. Otwinowski,Z. (1991) Isomorphous refinement and anomalous scattering. In *Proceedings of the CCP4 Study Weekend*, Warrington, UK, pp. 80–86.
30. Cowtan,K. (1994) Joint CCP4 and ESF-EACBM Newsletter on Protein Crystallography. **31**, 34.
31. Lamzin,V.S. and Wilson,K.S. (1993) Automated refinement of protein models. *Acta Crystallogr. D Biol. Crystallogr.*, **49**, 129–147.
32. Jones,T.A., Zou,J.Y., Cowan,S.W. and Kjeldgaard,M. (1991) Improved methods for building protein models in electron density maps and the location of errors in these models. *Acta Crystallogr. A*, **47**(Pt 2), 110–119.
33. Winn,M.D., Isupov,M.N. and Murshudov,G.N. (2001) Use of TLS parameters to model anisotropic displacements in macromolecular refinement. *Acta Crystallogr. D. Biol. Crystallogr.*, **57**, 122–133.
34. Holm,L. and Sander,C. (1993) Protein structure comparison by alignment of distance matrices. *J. Mol. Biol.*, **233**, 123–138.
35. Wu,L., Chan,K.L., Ralf,C., Bernstein,D.A., Garcia,P.L., Bohr,V.A., Vindigni,A., Janscak,P., Keck,J.L. and Hickson,I.D. (2005) The HRDC domain of BLM is required for the dissolution of double Holliday junctions. *EMBO J.*, **24**, 2679–2687.
36. Bernstein,D.A. and Keck,J.L. (2005) Conferring substrate specificity to DNA helicases: role of the RecQ HRDC domain. *Structure*, **13**, 1173–1182.
37. Jasiak,A.J., Armache,K.J., Martens,B., Jansen,R.P. and Cramer,P. (2006) Structural biology of RNA polymerase III: subcomplex C17/25 X-ray structure and 11 subunit enzyme model. *Mol. Cell*, **23**, 71–81.
38. Mattimore,V. and Battista,J.R. (1996) Radioresistance of Deinococcus radiodurans: functions necessary to survive ionizing radiation are also necessary to survive prolonged desiccation. *J. Bacteriol.*, **178**, 633–637.
39. Delano,W.L. (2002) *The PyMol Molecular Graphics System*. DeLano Scientific, San Carolos, CA.